International Journal of Power Electronics and Drive System (IJPEDS)
Vol. 17, No. 1, March 2026, pp. 58~68
ISSN: 2088-8694, DOI: 10.11591/ijpeds.v17.i1.pp58-68

Optimal speed control of SRM with integration of switching variable proportional desaturation fuzzy logic regulator for EV application

Kadali Ravi Kumar[1], Narender Jatoth[2], Shaik Mohammed Mukassir[3]
[1]Department of Electrical and Electronics Engineering, Vasavi College of Engineering (A), affiliated to Osmania University, Hyderabad, India
[2]Department of Electrical and Electronics Engineering, Princeton Institute of Engineering and Technology for Women, Hyderabad, India
[3]Department of Electrical and Electronics Engineering, Deccan College of Engineering and Technology, Hyderabad, India

Article Info

Article history:

Received Jun 24, 2025
Revised Nov 3, 2025
Accepted Dec 11, 2025

Keywords:

Electric vehicle
Proportional integral
SVPDFL
SVPDPI
Switched reluctance machine

ABSTRACT

SRMs are recognized for their high efficiency, strong torque output, and capability to operate at high speeds, making them well-suited for electric vehicle (EV) applications. Their high initial torque effectively overcomes the vehicle's inertia during the drive mode, enhancing overall performance. Switched reluctance machines (SRMs) come in various structural configurations such as 8/6, 6/4, and 4/2, offering flexible options for different vehicle requirements. Speed control in SRMs is typically managed through current regulation, which is handled by a current controller. Traditionally, a proportional integral (PI) controller is used to generate the required reference current. However, the PI regulator is prone to high damping and sensitivity to disturbances, leading to increased speed overshoot during startup and longer settling times. To address these limitations, a switched variable proportional desaturation PI (SVPDPI) controller is employed. Nevertheless, due to its relatively slow response, the PI component in the SVPDPI is replaced with a fuzzy logic module to enhance controller performance. This results in a switched variable proportional desaturation fuzzy logic (SVPDFL) regulator, which significantly reduces initial speed overshoot and improves settling time toward the desired reference speed. This paper presents a comparative analysis of these controllers, with simulations conducted using MATLAB/Simulink to evaluate performance improvements.

Corresponding Author:

Kadali Ravi Kumar
Department of Electrical and Electronics Engineering
Vasavi College of Engineering (A), affiliated to Osmania University
Approved by AICTE, New Delhi
9-5-81, Ibrahimbagh, Hyderabad - 500031, Telangana, India
Email: drkadaliravikumar@gmail.com

1. INTRODUCTION

Due to the rising environmental pollution caused by the combustion of fossil fuels such as petrol and diesel in transportation, the frequency of climate-related disasters is increasing globally. To prevent further environmental damage, it is essential to replace conventional internal combustion engine vehicles with zero-emission alternatives [1]. This shift can be effectively achieved through the adoption of electric vehicles (EVs), which operate entirely on electrical energy stored in onboard batteries [2]. These batteries power the electric motor, which drives the vehicle. Various types of electric machines can be used for traction in EVs, including induction machines, permanent magnet synchronous motors (PMSMs), and direct current (DC)

machines. However, these machines come with certain limitations, such as low starting torque, limited speed range, or high torque ripple. To address these challenges, the switched reluctance machine (SRM) is considered a suitable choice for EV drive applications. Table 1 highlights the advantages of SRM compared to induction machines and PMSMs [3].

Given these advantages, the SRM is highly suitable for EV applications. Its robust construction, high temperature tolerance, and cost-effectiveness enhance the overall reliability of the vehicle [4], [5]. For efficient operation, the speed of the SRM must be controlled while maintaining stable torque and minimizing the initial current peak and overshoot. This is achieved through current control using a power converter connected to the SRM. In this setup, the SRM is interfaced with the EV battery pack via three active hybrid bridges (AHBs), each configured with insulated gate bipolar transistor (IGBT) and diode switches in a full-bridge arrangement [5], [6]. The integration of the SRM with AHBs and the current control strategy is illustrated in Figure 1.

As illustrated in Figure 1, the battery pack supplies power to the AHBs, which are controlled by a feedback controller. This controller generates gate pulses for the AHB switches (S1–S6) based on the rotor pole position detected by the 'Position Detector' module [7]. The switching of the AHBs is synchronized with the rotor position and governed by the reference speed set within the controller. In conventional speed control schemes, a proportional-integral (PI) regulator is typically used to generate the reference current (I_{ref}). However, due to the underdamped nature of the PI regulator, the system experiences significant initial current overshoot and oscillations, which result in increased settling time and potential stress or damage to the motor [8].

To address these limitations, the traditional PI regulator is replaced with a switched variable proportional desaturation PI (SVPDPI) regulator. This improves current stability by reducing peak overshoot and decreasing the settling time [9]. However, since SVPDPI still incorporates a proportional integral (PI) component, it suffers from a relatively slow dynamic response [10]. To enhance responsiveness, this paper proposes an upgraded version of SVPDPI by integrating a fuzzy logic (FL) regulator, forming the switched variable proportional desaturation fuzzy logic (SVPDFL) controller [11]. The FL regulator employs a set of membership functions (MFs) and a rule base to dynamically generate the required reference signal, enabling faster and more adaptive control performance under varying system conditions [12].

This paper is structured as follows: i) Section 1 presents an introduction to the proposed SRM-integrated EV architecture; ii) Section 2 details the modelling of the proposed system along with the design of the speed controller; iii) Section 3 focuses on the development of the SVPDFL regulator for speed control, including the complete internal structure and rule base of the fuzzy logic module; iv) Section 4 provides a comprehensive analysis of the simulation results obtained using MATLAB Simulink, evaluating the performance of the proposed regulators; and v) Finally, section 5 concludes the paper by validating the effectiveness of the SVPDFL regulator as an optimal controller for SRM speed control. References cited throughout the paper are listed after section 5.

Table 1. Machine type comparison table

Parameter	SRM	Induction motor	PMSM
Rotor complexity	Very simple (no windings)	Moderate (squirrel cage)	Complex (magnets)
Cost	Low	Moderate	High (due to rare-earth)
Efficiency (Wide range)	High	Moderate	High
Temperature tolerance	High	Moderate	Low (magnet degradation)
Fault tolerance	Excellent	Poor	Poor

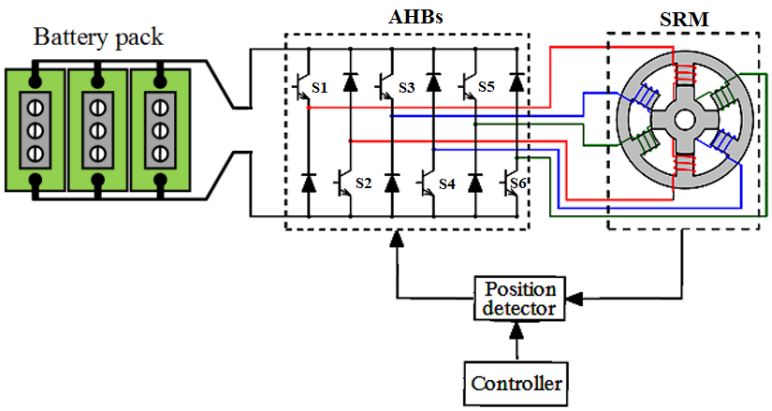

Figure 1. Structure of SRM integration into EV

2. PROPOSED SYSTEM

As described in section 1, the speed control of the SRM for EV applications is achieved through current regulation of the stator phases. To operate the switches of the AHBs, it is essential to determine the rotor position [13]. Based on the rotor's position, gate pulses are generated to turn ON the switches connected to the corresponding stator pole windings. Once the rotor position is identified, the reference current amplitude required for stator pole excitation is computed [14]. This reference current is generated by the speed regulator, which calculates the appropriate value based on the difference between the reference and measured speeds. The complete control structure of the SRM speed controller, including the current reference generator and position sensor, is illustrated in Figure 2.

As shown in Figure 2, the position of each stator pole is detected using a position sensor, which is essential for generating pulse signals to control the switches in the asymmetric half bridge (AHB) [15]. The internal configuration of this position sensor is illustrated in Figure 3. As shown in Figure 3, the input to the position sensor is the measured speed of the SRM (ω rad/sec). This speed is converted into degrees to determine the rotor's angular position (α°) [16]. The position angles corresponding to the three rotor phase poles are given as (1)-(3).

$$\theta_a = mod(90^0, \int \alpha^0) \tag{1}$$

$$\theta_b = mod(90^0, \int \alpha^0 - 30^0) \tag{2}$$

$$\theta_c = mod(90^0, \int \alpha^0 - 60^0) \tag{3}$$

The calculated rotor phase angles for each pole are compared against a defined angular range. A trigger signal is generated only when the rotor angle of any phase lies between 40° and 75°. This trigger signal is then multiplied by the reference current from the speed regulator, indicating the rotor position and activating the corresponding AHB switches for that phase. The reference current generated by the PI-based speed regulator is given as (4).

$$I_{ref} = (\omega^* - \omega)\left(k_p + \frac{k_i}{s}\right) \tag{4}$$

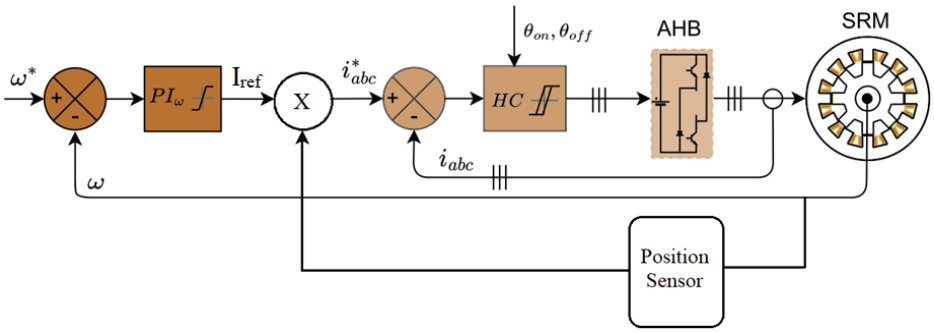

Figure 2. Speed control structure of SRM

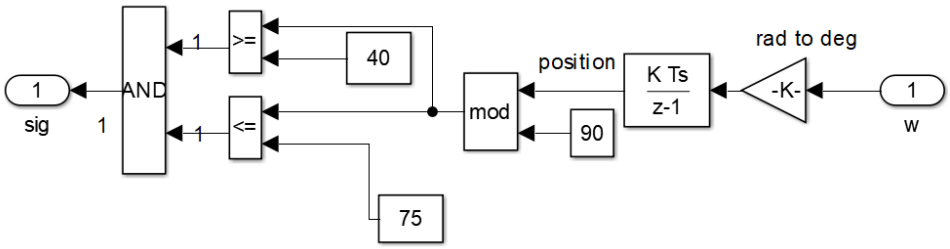

Figure 3. Position sensor internal structure

In (4), the reference speed (ω*) is compared with the measured speed (ω) to produce a speed error [17]. This error is processed by a PI controller, which uses proportional gain (k_p) and integral gain (k_i), both tuned based on the system's dynamic response. While the PI regulator is known for its reliability, low cost, simplicity, and ease of implementation, it suffers from low damping, resulting in higher oscillations and peak overshoots in the output signals. Moreover, the PI controller struggles to maintain stable operation under external transients, disturbances, and non-linearities, limiting its effectiveness to only stable system models [18]. The integral gain saturation further restricts its performance, especially in non-linear systems. Due to its lack of adaptability to system variations and error dynamics, the traditional PI regulator is unsuitable for complex environments with frequent disturbances. To achieve better control over the SRM characteristics, it becomes necessary to replace the PI regulator with more advanced adaptive regulators. A comparison table between some categories of the controllers is presented in Table 2.

Table 2. Controller type comparison table

Category	PI	Fuzzy logic	Sliding PI	Fuzzy-PI
Type	Feedback linear control	Fuzzy rule-based non-linear control	Variable gain structure	Hybrid (rule-based variable gain) control
Adaptability	No adaptability (fixed gains)	Good adaptability	Medium adaptability	Optimal adaptability
Robustness during dynamic states	Very low	Moderate	High	Very high
Response time	Low	Moderate	Good	Optimal
Damping	Very low damping	Medium damping	High damping	Critical damping
Sensitivity to disturbances	Medium	Lower	High	Mitigated

3. SWITCHING VARIABLE PROPORTIONAL DESATURATION FUZZY LOGIC REGULATOR

In order to improve the performance of the SRM for EV applications, the SRM speed controller needs to be enhanced with adaptive regulators [19]. This enhancement needs to improve the speed and torque characteristics of the machine when operated with the same rating of the system. To achieve this SVPDPI regulator is integrated into the SRM speed controller, which generates the reference current value [20], [21]. The internal structure of the SVPDPI regulator is presented in Figure 4.

The input to the SVPDPI regulator in the speed error (w_e) is generated by comparison of the reference and measured speed of the SRM. The output reference current of the regulator is expressed as (5)-(7).

$$If\ w_e \le s;\ I_{ref} = \begin{cases} w_e * \left(K_{P1} + \gamma \frac{Ki}{s}\right); If\ w_e > c\ and\ w_e > \varphi \\ w_e * \left(K_{P1} + \frac{Ki}{s}\right); If\ w_e > c\ and\ w_e \le \varphi \\ w_e * \left(K_{P2} + \gamma \frac{Ki}{s}\right); If\ w_e \le c\ and\ w_e > \varphi \\ w_e * \left(K_{P2} + \frac{Ki}{s}\right); If\ w_e \le c\ and\ w_e \le \varphi \end{cases} \quad (5)$$

$$If\ w_e > s;\ I_{ref} = w_e * \left(K_{P3} + \frac{Ki}{s}\right) \quad (6)$$

Here,

$$w_e = \omega^* - \omega \quad (7)$$

In (5) and (6), the K_{P1}, K_{P2} and K_{P3} are three different proportional gains, Ki is the integral gain, γ is the feedback compensation coefficient, φ and c are the threshold values, and 'S' is the selection coefficient [22]. These values are tuned as per the response of the system for the given reference value in the speed controller. However, in the structure of the SVPDPI regulator, due to the presence of the traditional PI regulator during $w_e > s$ condition, the response time of the regulator is restricted due to the underdamping of the PI regulator. This issue of the regulator is solved by replacing the traditional PI regulator with a fuzzy logic regulator during $w_e > s$ condition [23]. The updated SVPDFL regulator with fuzzy rules is presented in Figure 5.

As shown in Figure 5, the fuzzy logic module receives two input variables: the speed error (w_e) and the change in speed error (cw_e). The change in speed error is computed using a derivative block that calculates the difference between the current and previous values of the speed error [24]. Each input variable is fuzzified using seven membership functions (MFs), defined within specific ranges based on their respective minimum and maximum limits. The MFs are designed with a Gaussian ('gauss') shape to provide smoother transitions and enhanced flexibility across a wider operating range. The membership functions for the input variables 'w_e' and 'cw_e' are illustrated in Figures 6(a) and 6(b), respectively.

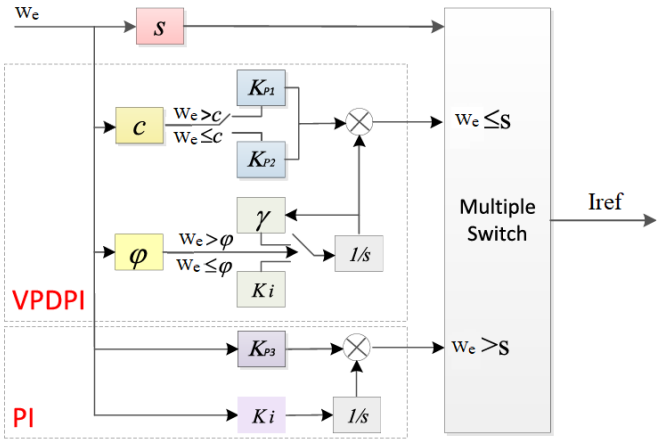

Figure 4. SVPDPI regulator internal structure

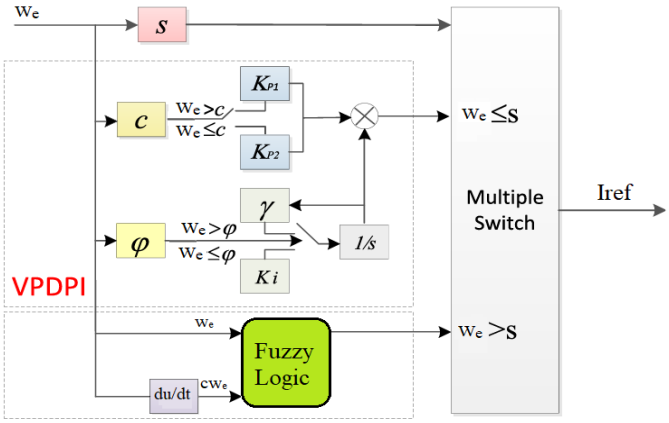

Figure 5. SVPDFL regulator internal structure

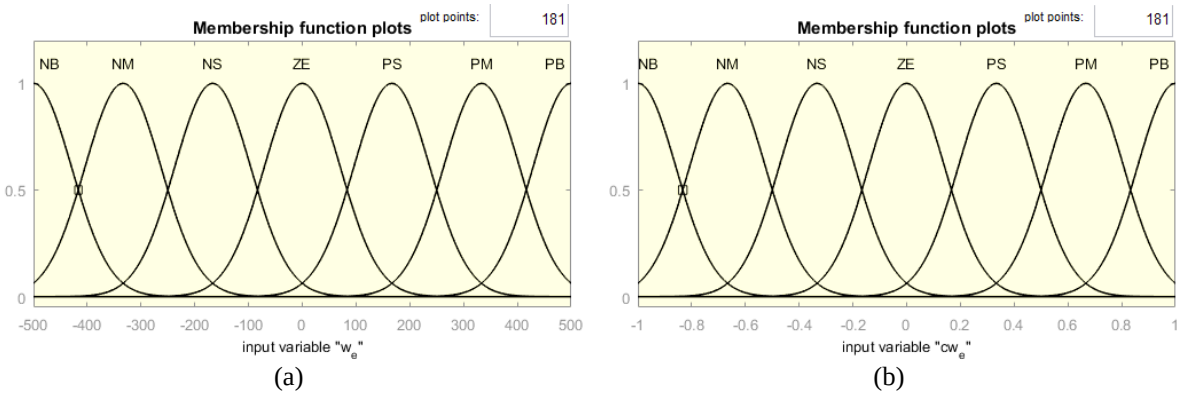

Figure 6. Fuzzy logic variables: (a) input variable 'w_e' MFs and (b) input variable 'cw_e' MFs

The membership functions (MFs) for the input variable 'w_e' are defined within the range of -500 to 500, representing the minimum and maximum speed error values. This reduced speed range is selected to enable a faster response from the controller. The MFs for the input variable 'cw_e' are set between -1 and 1, reflecting the typical minimum and maximum values produced by the derivative. Additionally, the output variable 'I_{ref}' is defined using seven triangular MFs to ensure precise output value generation. Figure 7 illustrates the MFs of the output variable.

As observed, the output variable 'I_{ref}' is defined within a range of -50 to 50, representing its minimum and maximum current values. The MFs for both input and output variables are named according to their position within this range [25]. On the negative side of the zero (ZE) MF, the functions are labelled as negative big (NB), negative medium (NM), and negative small (NS). On the positive side, they are labelled as positive small (PS), positive medium (PM), and positive big (PB). The fuzzy logic module operates based on a rule base consisting of 49 rules, as detailed in Table 3.

Based on the provided table, the output of the fuzzy logic module is generated according to the input signal range and the defined rule base. The updated SVPDFL regulator is then integrated into the SRM speed controller, and the resulting machine characteristics are analyzed and compared through simulation in the following section.

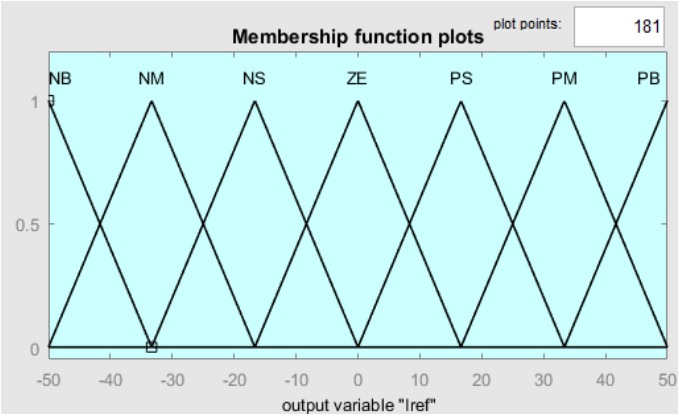

Figure 7. Output variable 'I_{ref}' MFs

Table 3. Rule base

49 rule-based		w_e						
		NB	NM	NS	ZE	PS	PM	PB
cw_e	PB	Z	PS	PM	PB	PB	PB	PB
	PM	NS	Z	PS	PM	PB	PB	PB
	PS	NB	NS	Z	PS	PM	PB	PB
	ZE	NB	NM	NS	Z	PS	PM	PB
	NS	NB	NB	NM	NS	Z	PS	PM
	NM	NB	NB	NB	NM	NS	Z	PS
	NB	NB	NB	NB	NB	NM	NS	Z

4. RESULT ANALYSIS

The proposed system, incorporating SRM speed control with various regulators, is modelled in the MATLAB Simulink environment. All modules are developed using blocks from the 'Electrical' subset of the Simulink library browser. The AHB switches are selected from the 'Power Electronics' section, the SRM is sourced from 'Machines', and the controller components are taken from 'Commonly Used Blocks' and 'Signal Routing'. Each block is configured with parameters specified in Table 4. The simulation model is run with a fixed initial speed using the updated parameters, and the results obtained with different speed regulators are recorded and presented with respect to time.

Table 4. Configuration parameters

Name of the module	Parameters
DC source	Vdc = 240 V
AHB	R_{igbt} = 1 mΩ, R_{diode} = 1 mΩ
SRM	Type: 6/4, R_s = 0.05Ω, J = 0.05 kg.m^2, F = 0.02 N.m.s, Unaligned inductance = 0.67 mH, aligned Inductance = 23.62 mH, Saturated aligned inductance = 0.15 mH, I_{max} = 65 A, Φ = 0.4 V.s
Position sensor	Lower limit = 40°, Upper limit = 75°
Speed control	PI regulator: K_p = 10; K_i = 0.5
	SVPDPI: K_{p1} = 0.1, K_{p2} = 1, γ = -14, K_i = 0.1, K_{p3} = 0.023, K_{i1}=0.05, c = 230, φ = 100, s = 50

Figure 8 shows the position sensor trigger signals generated by comparison of three rotor pole angles with the given range. It can be seen that each pulse is 120 deg phase shift to each other. Figure 9 is the reference current signal comparison of PI, SVPDPI, and SVPDFL regulators.

The initial peak of the I_{ref} of the PI regulator is very high, which leads to increased settling time. Compared to PI regulator, the SVPDPI and SVPDFL regulators, I_{ref} signals have reduced initial overshoot and also the settling time. The initial peak overshoot of PI regulator is observed to be 8000, SVPDPI and SVPDFL regulator is 50. Settling time is noted to be 0.38 sec for PI regulator, 0.28 sec for the SVPDPI regulator, and 0.12 sec for the SVPDFL. Along with the initial peak overshoot and settling time, the ripple in the I_{ref} signal is also less for the proposed regulators.

Figure 10 presents the rules of the fuzzy logic module with input (e and ce) and output (Iref) variables. The output of the fuzzy logic module is integrated into the SVPD regulator for adaptive control over the speed of the SRM. As the initial peak of the reference current for the PI regulator is high the torque of SRM is also very high at 1100 Nm, which can damage the machine. Limiting the reference current using adaptive desaturation regulators is necessary for control over the initial torque of the machine to avoid uncertainties. Figure 11 represents the SRM electromagnetic torque, which shows the initial value of the SVPDPI and SVPDFL regulators to be 70 Nm.

Figure 12 is the comparison of flux of the SRM, which can be observed to be in given limits with a maximum flux value of 0.3 V.s. After the speed settles to the reference desired value, the flux drops to 0.1 V.s and maintains the same throughout the simulation. After the speed settles, the flux magnitude is maintained the same for all the regulators. As observed in Figure 13, the speed of the SRM with the SVPDFL regulator integrated SRM speed controller has no overshoot and a lower settling time as compared to PI and SVPDPI regulators. A parameter comparative table with SRM characteristics is presented in Table 5.

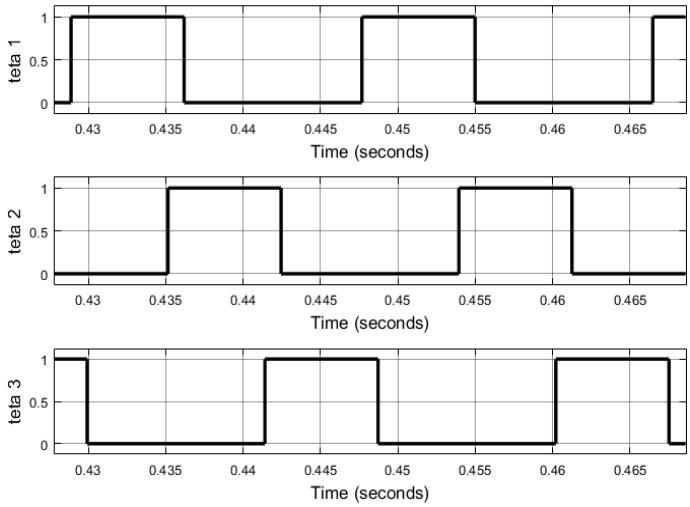

Figure 8. Position sensor trigger signals

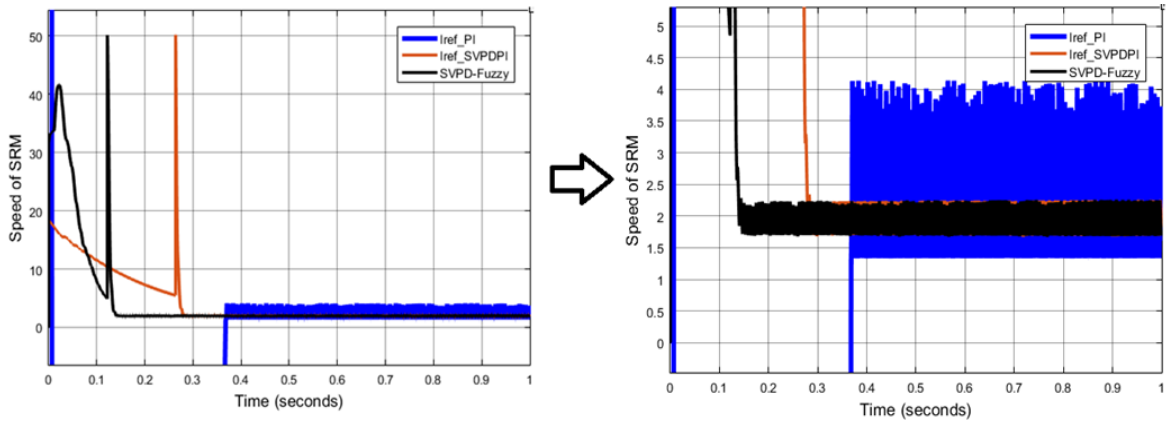

Figure 9. I_{ref} signal generated by regulators (a) full simulation time plot and (b) zoomed plot

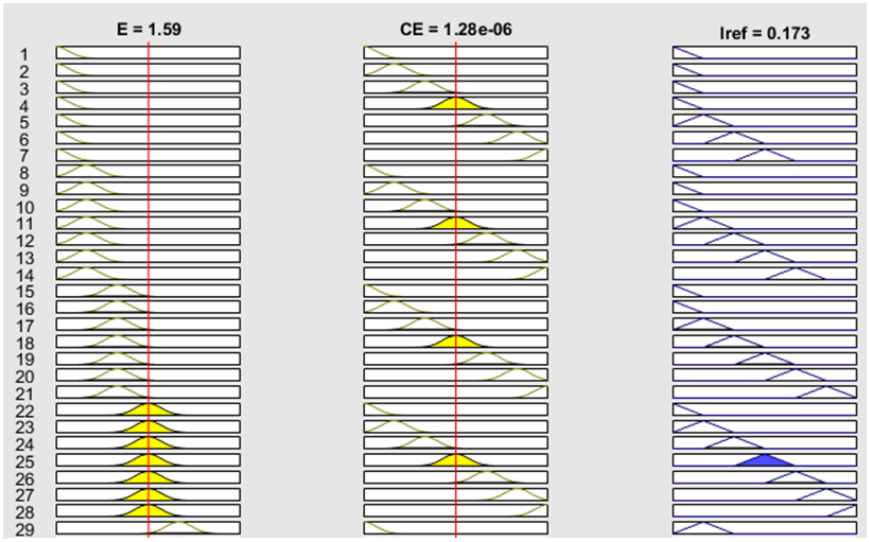

Figure 10. Fuzzy output with respect to the rule base

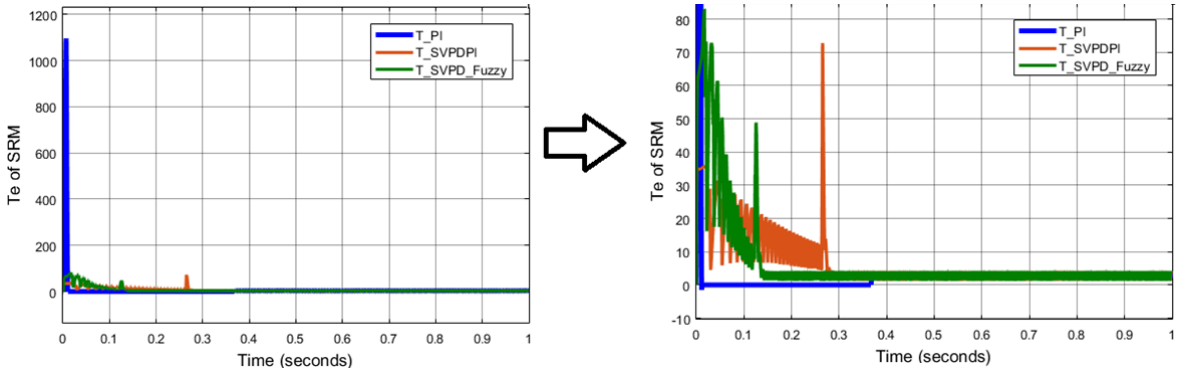

Figure 11. Comparison of electromagnetic torque of SRM: (a) full simulation time plot and (b) zoomed plot

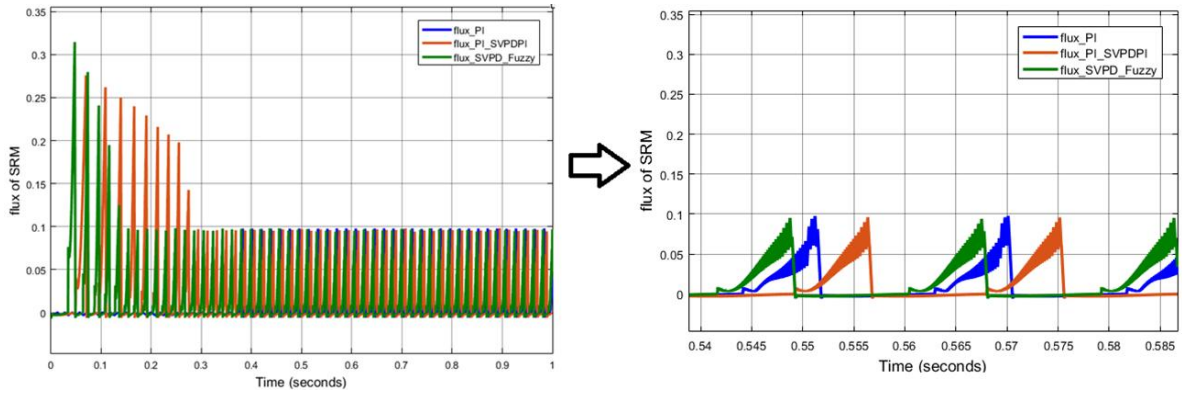

Figure 12. Comparison of flux of SRM: (a) full simulation time plot and (b) zoomed plot

Table 5. Comparison table

Name of the parameter	PI	SVPDPI	SVPDFL
Iref peak	8000 A	50 A	50 A
Iref ripple	60%	20%	20%
Te peak	1100 Nm	70 Nm	70 Nm
Te settling time	0.38 sec	0.28 sec	0.12 sec
Speed peak	1020 rpm	No peak	No peak
Speed settling time	0.35 sec	0.28 sec	0.12 sec

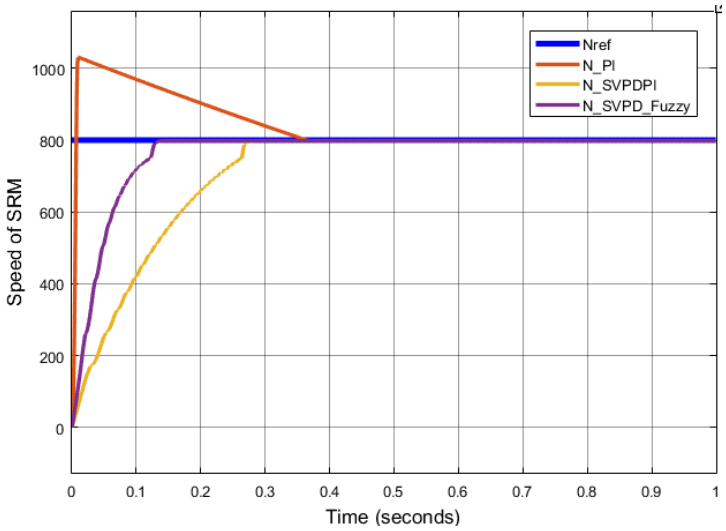

Figure 13. Comparison of SRM speeds

5. CONCLUSION

The speed control of the SRM is implemented in the MATLAB Simulink environment, with performance analysis conducted through graphical representations. Initially, the use of a conventional PI regulator resulted in an underdamped response, causing significant initial peaks and ripples in the SRM's current, torque, and speed. To address this issue, the PI regulator was replaced with an SVPDPI regulator, which enhanced damping and controller responsiveness, thereby reducing peak overshoot in these parameters. However, since the SVPDPI regulator still incorporates a traditional PI component, the improvement in response time was limited. To overcome this limitation, the traditional PI regulator was replaced with a fuzzy logic module within the SVPDPI structure. This modification significantly enhanced the controller's response time, eliminating overshoots and ensuring faster settling of the SRM speed. The graphical results confirm improved machine performance, with reduced current peaks and torque ripples, thereby increasing system reliability.

FUNDING INFORMATION

Authors state no funding involved.

AUTHOR CONTRIBUTIONS STATEMENT

This journal uses the Contributor Roles Taxonomy (CRediT) to recognize individual author contributions, reduce authorship disputes, and facilitate collaboration.

Name of Author	C	M	So	Va	Fo	I	R	D	O	E	Vi	Su	P	Fu
Kadali Ravi Kumar	✓	✓	✓	✓	✓	✓	✓		✓	✓	✓	✓	✓	
Narender Jatoth	✓	✓	✓	✓	✓	✓	✓	✓	✓	✓				
Shaik Mohammed Mukassir	✓	✓	✓	✓	✓	✓	✓	✓	✓	✓	✓		✓	

C : **C**onceptualization
M : **M**ethodology
So : **So**ftware
Va : **Va**lidation
Fo : **Fo**rmal analysis
I : **I**nvestigation
R : **R**esources
D : **D**ata Curation
O : Writing - **O**riginal Draft
E : Writing - Review & **E**diting
Vi : **Vi**sualization
Su : **Su**pervision
P : **P**roject administration
Fu : **Fu**nding acquisition

CONFLICT OF INTEREST STATEMENT

Authors state no conflict of interest.

DATA AVAILABILITY

The authors confirm that the data supporting the findings of this study are available within the article [and/or its supplementary materials].

REFERENCES

[1] J. Morfeldt, S. Davidsson Kurland, and D. J. A. Johansson, "Carbon footprint impacts of banning cars with internal combustion engines," *Transportation Research Part D: Transport and Environment*, vol. 95, p. 102807, Jun. 2021, doi: 10.1016/j.trd.2021.102807.

[2] N. Ha, "Comparative environmental impacts of Internal combustion engine vehicles with hybrid vehicles and electric vehicles in China—Based on life cycle assessment," in *2019 4th International Conference on Advances in Energy and Environment Research (ICAEER 2019)*, 2019. doi: 10.1051/e3sconf/201911802010.

[3] S. Krishnamoorthy and P. P. K. Panikkar, "A comprehensive review of different electric motors for electric vehicles application," *International Journal of Power Electronics and Drive Systems (IJPEDS)*, vol. 15, no. 1, p. 74, Mar. 2024, doi: 10.11591/ijpeds.v15.i1.pp74-90.

[4] R. Bhattacharjee, "Switched reluctance motor applications to EV and HEV: Torque control issues," in *2014 1st International Conference on Non Conventional Energy (ICONCE 2014)*, Jan. 2014, pp. 324–328. doi: 10.1109/ICONCE.2014.6808735.

[5] B. Srinivasulu, G. V. Nagesh Kumar, V. Rafi, and P. Nageswara Rao, "Optimal design of SRM for EV application," *Journal of Physics: Conference Series*, vol. 2070, no. 1, p. 012140, Nov. 2021, doi: 10.1088/1742-6596/2070/1/012140.

[6] S. Krishnamoorthy and P. P. K. Panikkar, "Modified switching control of SRM drives for electric vehicles application with torque ripple reduction," *International Journal of Power Electronics and Drive Systems*, vol. 15, no. 1, pp. 147–159, 2024, doi: 10.11591/ijpeds.v15.i1.pp147-159.

[7] W.-K. Gu, C.-W. Yang, and C.-M. Liaw, "An EV SRM drive and its interconnected operations integrated into grid, microgrid, and vehicle," *Applied Sciences*, vol. 14, no. 7, p. 3032, Apr. 2024, doi: 10.3390/app14073032.

[8] H. Cheng, Z. Wang, S. Yang, J. Huang, and X. Ge, "An integrated SRM powertrain topology for plug-in hybrid electric vehicles with multiple driving and onboard charging capabilities," *IEEE Transactions on Transportation Electrification*, vol. 6, no. 2, pp. 578–591, 2020, doi: 10.1109/TTE.2020.2987167.

[9] G. V. Kumar, C. H. Chuang, M. Z. Lu, and C. M. Liaw, "Development of an electric vehicle synchronous reluctance motor drive," *IEEE Transactions on Vehicular Technology*, vol. 69, no. 5, pp. 5012–5024, 2020, doi: 10.1109/TVT.2020.2983546.

[10] Z. Wei, M. Zhao, X. Liu, and M. Lu, "Speed control for SRM drive system based on switching variable proportional desaturation PI regulator," *IEEE Access*, vol. 9, pp. 69735–69746, 2021, doi: 10.1109/ACCESS.2021.3078194.

[11] A. Rajendran and B. Karthik, "Design and analysis of fuzzy and PI controllers for switched reluctance motor drive," *Materials Today: Proceedings*, vol. 37, pp. 1608–1612, 2021, doi: 10.1016/j.matpr.2020.07.166.

[12] R. M. Abdel-Fadil and L. Számel, "Direct instantaneous torque control of the switched reluctance motor for electric vehicles applications using fuzzy logic control," *Acta Technica Jaurinensis*, vol. 12, no. 2, pp. 101–116, 2019, doi: 10.14513/actatechjaur.v12.n2.496.

[13] T. Pourseif and M. Mohajeri, "Design of robust control for a motor in electric vehicles," *IET Electrical Systems in Transportation*, vol. 10, no. 1, pp. 68–74, 2020, doi: 10.1049/iet-est.2018.5084.

[14] S. Suresh, J. Peter, and V. Chellappan, "Mathematical modeling and speed control of 6/4 switched reluctance motor drive," in *2022 International Conference on Futuristic Technologies in Control Systems & Renewable Energy (ICFCR)*, Jul. 2022, pp. 1–6. doi: 10.1109/ICFCR54831.2022.9893644.

[15] L. Senthil Murugan and P. Maruthupandi, "Sensorless speed control of 6/4-pole switched reluctance motor with ANFIS and fuzzy-PID-based hybrid observer," *Electrical Engineering*, vol. 102, no. 2, pp. 831–844, Jun. 2020, doi: 10.1007/s00202-019-00915-5.

[16] D. S. Mihić, B. M. Brkovic, and M. V. Terzic, "Asymmetrical four-phase 8/6 switched reluctance motor for a wide constant power region," *Machines*, vol. 12, no. 7, p. 454, Jul. 2024, doi: 10.3390/machines12070454.

[17] Y. Zhang, L. Chen, Z. Wang, and E. Hou, "Speed control of switched reluctance motor based on regulation region of switching angle," *Energies*, vol. 15, no. 16, p. 5782, Aug. 2022, doi: 10.3390/en15165782.

[18] J. Zhang, C. Liu, S. Chen, and L. Zhang, "Research on speed control of switched reluctance motors based on improved super-twisting sliding mode and linear active disturbance rejection control," *Electronics*, vol. 14, no. 6, p. 1065, Mar. 2025, doi: 10.3390/electronics14061065.

[19] Y. Eldigair, F. Garelli, C. Kunusch, and C. Ocampo-Martinez, "Adaptive PI control with robust variable structure anti-windup strategy for systems with rate-limited actuators: Application to compression systems," *Control Engineering Practice*, vol. 96, p. 104282, Mar. 2020, doi: 10.1016/j.conengprac.2019.104282.

[20] S. C. Song, B. N. Qu, and J. C. Song, "Application of variable gain PI controller in switched reluctance motor," *Miniature Special Motor*, vol. 45, no. 8, pp. 61–64, 2017.

[21] H. Chu, D. Yue, C. Dou, and L. Chu, "Adaptive PI control for consensus of multiagent systems with relative state saturation constraints," *IEEE Transactions on Cybernetics*, vol. 51, no. 4, pp. 2296–2302, Apr. 2021, doi: 10.1109/TCYB.2019.2954955.

[22] K. Radha Rani, S. K. Salma, A. Raghunath, and K. Praveen Kumar, "Comparative study of speed control of 6/4 switched reluctance motor using Hybrid fuzzy logic controller," *International Journal of Control Theory and Applications*, vol. 8, no. 1, pp. 259–269, 2015.

[23] R. S. Ambhore, Y. B. Mandake, and D. S. Bankar, "Simulation and analysis of performance of SRM by using different controller," *Indian Journal of Science and Technology*, vol. 16, no. 25, pp. 1910–1917, Jul. 2023, doi: 10.17485/IJST/v16i25.1166.

[25] Z. Omaç, "Fuzzy-logic-based robust speed control of switched reluctance motor for low and high speeds," *Turkish Journal of Electrical Engineering and Computer Sciences*, vol. 27, no. 1, pp. 316–329, 2019, doi: 10.3906/elk-1712-186.

BIOGRAPHIES OF AUTHORS

Dr. Kadali Ravi Kumar is a professor in the Department of Electrical and Electronics Engineering at Vasavi College of Engineering (A), Hyderabad, affiliated with Osmania University, India. He earned his Ph.D. in Electrical Engineering with a specialization in Power Systems from the National Institute of Technology (NIT) Warangal. He has extensive teaching and research experience, with numerous publications in reputed national and international journals and conferences. His areas of interest include power system control, optimization, FACTS devices, smart grid technologies, renewable energy integration, and intelligent systems in electrical engineering. He is currently supervising multiple Ph.D. research scholars, and many students have been awarded Ph.D. degrees under his esteemed guidance and supervision. He has also successfully guided several M.E. and B.E. students in their academic research projects. He has actively contributed to academic leadership by coordinating Faculty Development Programs (FDPs), Short-Term Training Programs (STTPs), and national and international conferences. He has been invited to address several academic events and has participated in various international conferences and advanced faculty development programs. He is widely recognized for his commitment to quality research, active mentoring, and academic excellence. He can be contacted at email: drkadaliravikumar@gmail.com.

Dr. Narender Jatoth is currently working as an assistant professor in the Department of Electrical Engineering at the Princeton Institute of Engineering & Technology for Women, Hyderabad. He obtained his Ph.D. in Electrical Engineering from the University College of Engineering, Osmania University, Hyderabad. He holds an M.Tech. in Power Electronics from Ramappa Engineering College (JNTUH) and a B.Tech. in Electrical and Electronics Engineering from J. B. Institute of Engineering and Technology (JNTUH). His doctoral research focused on soft-switched LED driver circuit configurations aimed at improving power conversion efficiency, reducing device current, and enhancing dimming control for lighting applications. He has over a decade of teaching experience and has published several research papers in reputed international journals on topics such as power quality, soft-switching converters, dynamic voltage restorers, and renewable energy systems. His research interests include power electronics, power quality improvement, and smart grid technologies. He can be contacted at email: narenderjatoth@gmail.com.

Dr. Shaik Mohammed Mukassir received his B.E. degree in Electrical and Electronics Engineering from Deccan College of Engineering and Technology, Hyderabad, affiliated with Osmania University, Telangana. He obtained his M.E. degree in Power Electronics Systems from the University College of Engineering, Osmania University, Hyderabad. He obtained his Ph.D. in Electrical Engineering from Osmania University, Hyderabad, Telangana, India. His research interests include power electronic converter applications for renewable energy systems, hybrid renewable energy integration, power quality improvement, microgrids, and LED driver circuit design. He has authored and co-authored several papers in peer-reviewed journals and international conferences indexed in Scopus. He has actively delivered, attended, and participated in numerous faculty development programs (FDPs), conferences, workshops, and webinars organized by IEEE and other academic institutions. He is also a member of several professional and technical bodies. He is currently serving as an assistant professor in the Department of Electrical and Electronics Engineering at Deccan College of Engineering and Technology, Nampally, Hyderabad, Telangana, India. He can be contacted at email: mukassir_be@yahoo.com.